Open Access Journal

Journal of Power Technologies 99 (1) (2019) 31–39

journal homepage:papers.itc.pw.edu.pl

The 48-Pulse VSC-Based Generalized Interline Power-Flow Controller (GIPFC)

Amir Ghorbani*

Department of Electrical Engineering, Science & Research Branch, Azad University, Tehran, Iran

Abstract

The generalized interline power-flow controller (GIPFC) is a voltage-source controller (VSC)-based flexible ac transmission system (FACTS) controller that can independently regularize the power-flow over each transmission line of a multiline system. This paper presents a modeling and performance analysis of GIPFC based on 48-pulsed voltage-source converters. This paper deals with a cascaded multilevel converter model, which is a 48-pulse (three levels) source converter. The voltage source converter described in this paper is a harmonic neutralized, 48-pulse GTO converter. The GIPFC controller is based on d-q orthogonal coordinates. The algorithm is verified using simulations in MATLAB/Simulink environment. Comparisons between Unified Power Flow Controller (UPFC) and GIPFC are also included.

Keywords: Flexible ac transmission system (FACTS); Generalized Interline Power-Flow Controller (GIPFC); Voltage Source Converter (VCS); 48-pulse GTO converter

1. Introduction

Flexible alternating current transmission system (FACTS) technology has opened up new opportunities in dynamic control of voltage, impedance and phase-angle of high voltage transmission lines. FACTS devices, which are used for power control, can be divided into two categories. The first includes devices which utilize transformers with thyristors and impedances to control the power (e.g. SVC, TCSC and etc.). The second category includes devices which utilize switching power supplies to build a controllable static synchronous voltage source (e.g. STATCOM, SSSC and UPFC). GIPFC is a new FACTS device which falls into the second category. The main advantage of GIPFC is its capability in controlling power over different transmission lines at the same time [1]. The general structure of GIPFC is shown in Fig. 1. It includes a shunt part (STATCOM) and two parts in series (SSSC). If all switches S1, S2 and S3 are closed the result will be a GIPFC. Flexibility in configuration is another advantage of GIPFC. Table 1 lists the different operating modes resulting from different switch settings.

It can be seen from Fig. 1 that three different Voltage Source Converters (VSCs) are utilized. Voltage Source Converters without additional AC filters can include higher order harmonics which are not acceptable from the system and robustness point of view (even with 24-pulse levels). In [2] 48-pulse converters are proposed which can be used without any supplementary AC filter. In this paper, 48-pulse converters are used in modeling the GIPFC. Different configurations and performance comparisons are included. The simulation results are verified with analytic studies discussed in [3].

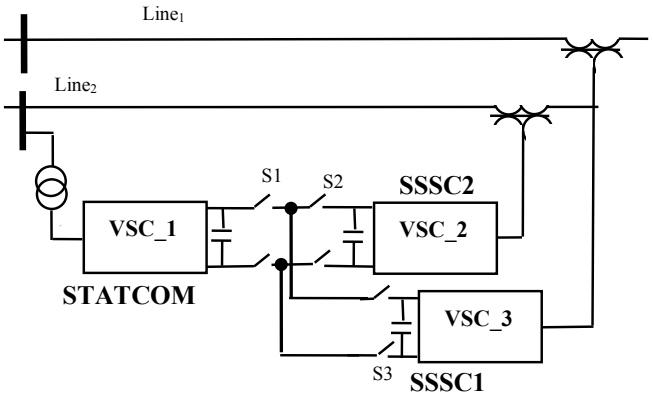

Figure 1: GIPFC model

Convertible and multi-purpose controllers are introduced by utilizing UPFC to increase transmission line performance [4, 5]. This type of controller, employing voltage source converters, can be used for voltage control, impedance compensation or angle compensation separately. They can also connect to a common DC link to utilize extensive capabilities of transmission power control (Fig. 1). It can

*Corresponding author

Email address: amirghorbani.elec@gmail.com, Tel: +989143434074 (Amir Ghorbani)

Table 1: FACTS achieved by different configurations of switches in Fig. 1

Case	State of Switches			FACTS
Number	S1	S2	S3	
1	Close	Close	Close	GIPFC
2	Close	Close	Open	UPFC + SSSC1
3	Open	Close	Close	IPFC+STATCOM
4	Close	Open	Close	UPFC + SSSC2
5	Open	Open	Open	STATCOM+SSSC1+SSSC2

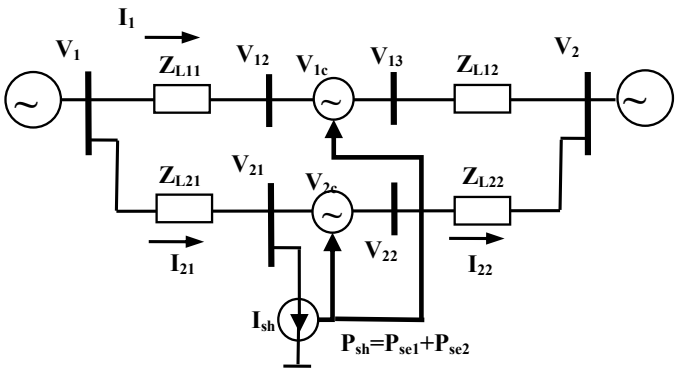

Figure 2: The model System

be seen from the figure that GIPFC is composed of two static synchronous series compensators (SSSC) and one shunt static synchronous compensator (STATCOM). When S1 is open, STATCOM will be used for voltage or reactive power control [6]. Two combined SSSC with a common DC link lead to an Interline Power Flow Controller (IPFC). The output voltage for one of the SSSCs has controllable magnitude and phase. The other SSSC is used for active power control. This combination can be used to control active power in multi-line systems, transferring load between high loaded and low loaded lines [7].

The first multi-line controller was IPFC [7], which was analyzed later in [8, 9, 10], investigates generalized UPFC in which the major factor model of GUPFC was used for stability analysis. In [3], an analytic method is proposed to study power transfer control using GIPFC. This analytic method is used to verify simulation results in this paper. GIPFC and UPFC are compared from the performance and limitations point of view using the proposed method.

2. GIPFC analysis

The system studied is shown in Fig. 2. The parameters are assumed to be the same for both lines. Using a steady state model based on d-q equations makes it easier to model ideal voltage sources. Accordingly, d-q coordinate equations are used in this paper. Current and voltage equations are as follows [3]:

$$\bar{I}_1 = \bar{I}_1^o + \bar{I}_1^c \tag{1}$$

In the equation above $\bar{I}_1^o$ represents the current for line 1 without compensation. $\bar{I}_1^c$ represents the current for line 1 that comes from V_{1C} compensator. Transmission lines resistance is assumed negligible, for simplicity. Supposing $X_{L1} = X_{L11} + X_{L12}$ and $X_{L2} = X_{L21} + X_{L22}$, we have:

$$\bar{I}_1^o = \left(\frac{V_{1q} - V_{2q}}{X_{L1}} - j\frac{V_{1d} - V_{2d}}{X_{L1}}\right) \tag{2}$$

Similarly, we have:

$$\bar{I}_1^c = \frac{\bar{V}_{1c}}{jX_{L1}} = \left(\frac{V_{1cq}}{X_{L1}} - j\frac{V_{1cd}}{X_{L1}}\right) \tag{3}$$

Substituting eq. (3) and eq. (2) at eq. (1), active and reactive power can be derived as follows:

$$\begin{aligned} P_1 &= P_1^o + (V_{2d}\tfrac{V_{1cq}}{X_{L1}} - V_{2q}\tfrac{V_{1cd}}{X_{L1}}) \\ Q_1 &= Q_1^o + (V_{2q}\tfrac{V_{1cq}}{X_{L1}} + V_{2d}\tfrac{V_{1cd}}{X_{L1}}) \end{aligned} \tag{4}$$

Q_1^o and $P_1^o$are reactive and active power when there is no compensation. We can repeat the same calculations for the second line. The only difference is the presence of I_{sh} which comes from STATCOM:

$$\begin{aligned} I_{21d} &= I_{22d}^o + \tfrac{V_{2cq}}{X_{L2}} + \tfrac{X_{L22}}{X_{L2}} I_{shd} \\ I_{21q} &= I_{22q}^o - \tfrac{V_{2cd}}{X_{L2}} + \tfrac{X_{L22}}{X_{L2}} I_{shq} \\ I_{22d} &= I_{22d}^o + \tfrac{V_{2cq}}{X_{L2}} - \tfrac{X_{L21}}{X_{L2}} I_{shd} \\ I_{22q} &= I_{22q}^o + \tfrac{V_{2cd}}{X_{L2}} - \tfrac{X_{L21}}{X_{L2}} I_{shq} \end{aligned} \tag{5}$$

So, d-q voltages of STATCOM bus or $\bar{V}_{21}$ is:

$$V_{21d} = V_{1d} + X_{L21} I_{21q}; \quad V_{21q} = V_{1q} - X_{L21} I_{21d} \tag{6}$$

The power for SSSC1 (series converter) is:

$$P_{se1} = V_{1cd} I_{1d} + V_{1cq} I_{1q} \tag{7}$$

Similarly, the power for SSSC2 is:

$$P_{se2} = V_{2cd} I_{22d} + V_{2cq} I_{22q} \tag{8}$$

Substituting eq. (5) in eq. (8) we have:

$$P_{se2} = \left[V_{2cd} I_{22d} + V_{2cq} I_{22q} - \frac{X_{L21}}{X_{L2}}(V_{2cd} I_{shd} + V_{2cq} I_{shq})\right] \tag{9}$$

For the parallel compensator we have:

$$P_{sh} = V_{21d} I_{shd} + V_{22q} I_{shq} \tag{10}$$

Substituting eq. (5) and eq. (6) in eq. (9) we have:

$$\begin{aligned} P_{sh} &= I_{shd}(V_{1d} + X_{L21} I_{22q}^o - \tfrac{X_{L21}}{X_{L2}} V_{2cd}) \\ &+ I_{shq}(V_{1q} + X_{L21} I_{22d}^o - \tfrac{X_{L21}}{X_{L2}} V_{2cq}) \end{aligned} \tag{11}$$

Neglecting inverter losses, it can be mentioned that the parallel converter supplies the power for both series converters:

$$P_{sh} = P_{se1} + P_{se2} \tag{12}$$

Substituting eq. (1), eq. (7), eq. (9) and eq. (11) at eq. (12) we have:

$$\begin{aligned} &\underbrace{(V_{1cd} I_{1d}^o + V_{1cq} I_{1q}^o) + (V_{2cd} I_{22d}^o + V_{2cq} I_{22q}^o)}_{d} \\ &-I_{shd}\underbrace{(V_{1d} + X_{L21} I_{22q}^o)}_{b} - I_{shq}\underbrace{(V_{1q} - X_{L21} I_{22d}^o)}_{b} = 0 \end{aligned} \tag{13}$$

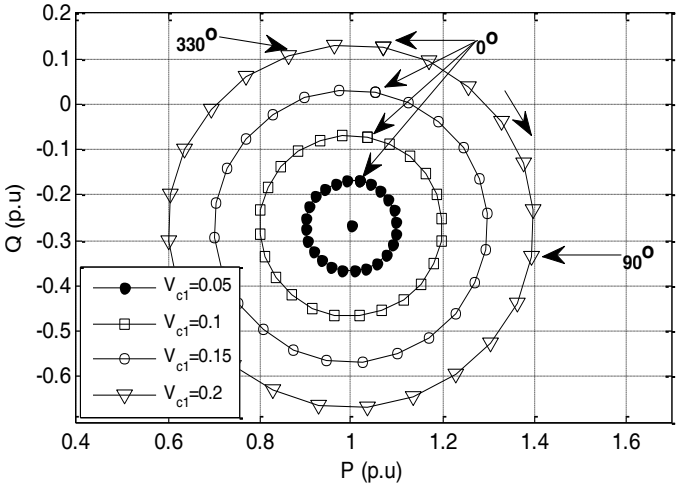

Figure 3: P-Q curve for SSSC1

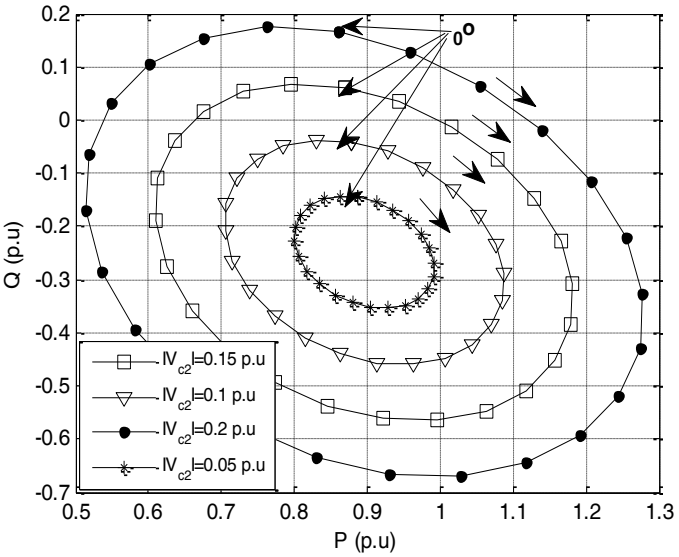

Figure 4: P-Q curve for SSSC2

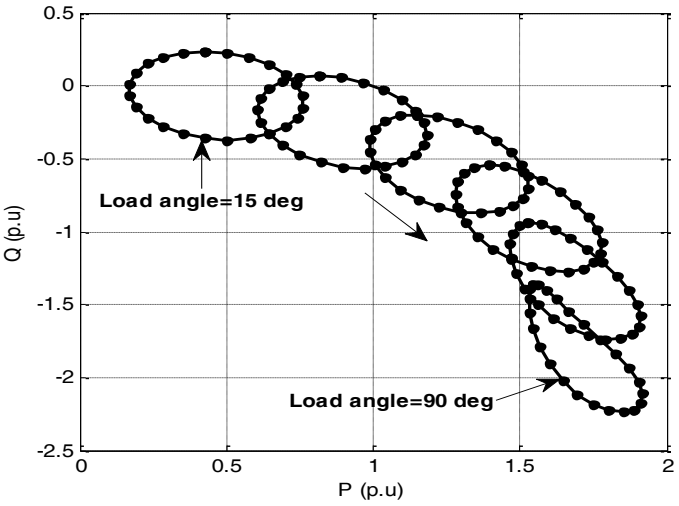

Figure 5: SSSC2 P-Q curve for different load angles

In other words:

$$d - bI_{shd} - aI_{shq} = 0 \tag{14}$$

The reactive power absorbed or supplied by STATCOM for controlling V_{21} is:

$$Q_{sh} = (V_{21q}I_{shd} - V_{21d}I_{shq}) \tag{15}$$

Substituting eq. (5) and eq. (6) at eq. (15) we have:

$$\begin{aligned} &k_1(I_{shd})^2 + (k_2V_{2cq} - a)I_{shd} + k_1(I_{shq})^2 \\ &-(k_2V_{2cd} - b)I_{shq} + c = 0 \end{aligned} \tag{16}$$

In which: $k_1 = X_{L21}X_{L22}/X_{L2}$, $k_2 = X_{L21}/X_{L2}$ and $c = Q_{sh}$. Using eq. (14) and eq. (16), parameters I_{shd} and I_{shq} can be obtained:

$$AI_{shd}^2 + BI_{shd} + C = 0 \tag{17}$$

In which A, B and C are as follows:

$$\begin{aligned} A &= k_1\left[1 + (\tfrac{b}{a})^2\right] \\ B &= k_2(V_{2cq} + \tfrac{b}{a}V_{2cd}) - (\tfrac{a^3+2bdk_1+ab^2}{a^2}) \\ C &= \tfrac{d}{a}(k_1\tfrac{d}{a} - k_2V_{2cd} + b + \tfrac{ac}{d}) \end{aligned} \tag{18}$$

The currents can be obtained using eq. (14) and eq. (18). Using the currents, active and reactive powers at the receiver can be derived as follows:

$$\begin{aligned} P_2 &= P_2^o + \tfrac{V_{2d}}{X_{L2}}(V_{2cq} - X_{L21}I_{shd}) - \tfrac{V_{2q}}{X_{L2}}(V_{2cd} - X_{L21}I_{shq}) \\ Q_2 &= Q_2^o + \tfrac{V_{2q}}{X_{L2}}(V_{2cq} - X_{L21}I_{shd}) + \tfrac{V_{2d}}{X_{L2}}(V_{2cd} + X_{L21}I_{shq}) \end{aligned} \tag{19}$$

P_2^o and Q_2^o are active and reactive powers of the second line when there is no compensation. In the next section a GIPFC operational analysis for difference working states is presented, based on P-Q curve analysis.

2.1. GIPFC operational analysis

To analyze GIPFC capability in controlling active and reactive power, a P-Q curve is used. The curve represents active and reactive power at the receiving end for different values of output voltage degrees, varying from 0 to 360 degrees. Fig. 3 shows the P-Q curve for different values of V_{1c} considering $V_{2c} = 0.15$. Inside the circles shown with P_1^o and Q_1^o as the centers are controllable regions of series converter SSSC1. The radius is proportional to the voltage injected by SSSC1. Fig. 4 shows the second line controllable region by SSSC2. $V_{1c} = 0.2$, angle = 15 degrees and $\delta = 30°$. It can be seen from the figure that the curves are not circles in this case. This is due to STATCOM, which is expected referring to eq. (19). P_1^o and Q_1^o are not at the center either for this case. Changing system load angle will change P_0 and Q_0 values and as a result the SSSC1 controllable area centered at P_0 and Q_0 will shift as well. It can be deduced from eq. (4) that line-1 is independent of line 2. The P-Q area remains the same for all load angle values. However, the P-Q region for line-2 will no longer be elliptical for higher values of load angle. Fig. 5 shows the SSSC2 P-Q curve for different values of load angle ($V_{1c} = 0.2$, angle = 15 degrees and $V_{2c} = 0.15$).

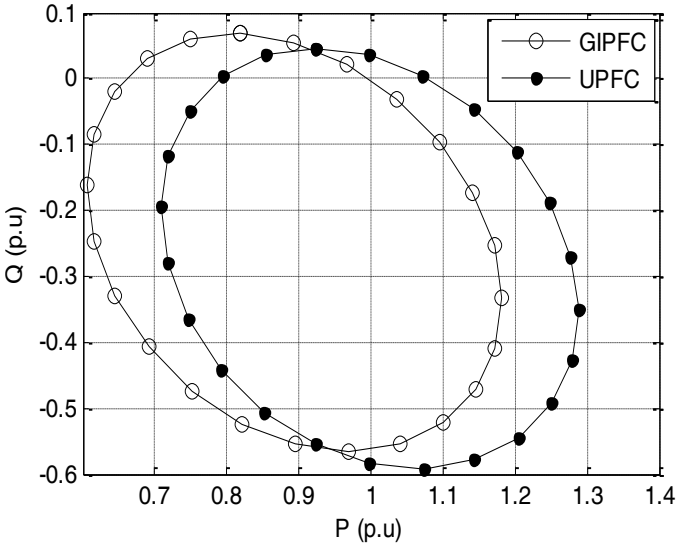

Figure 6: P-Q curve comparison between UPFC and GIPFC

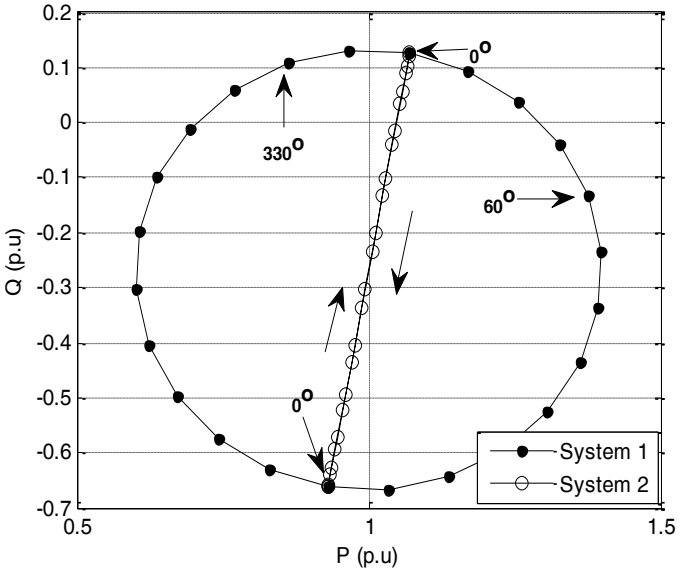

Figure 7: P-Q curve comparison between IPFC and GIPFC

2.2. Comparing GIPFC with UPFC and IPFC

Series converter SSSC1 is not utilized for UPFC. Fig. 6 shows UPFC and GIPFC P-Q comparison with $V_{1c} = 0.2$, $V_{2c} = 0.15$ and angle = 15 degrees in the case of GIPFC. It can be seen that the area remains the same and it only shifts in the P-Q plane.

IPFC usually contains multiple series compensators which are connected to each other in their DC terminals. Two SSSCs are considered for IPFC in our study. In this configuration, besides series reactive compensation, each converter can be used to supply active power from the transmission line into its common DC link [5]. For IPFC, the shunt part of GIPFC (STATCOM) is not in use, which means $Q_{sh} = 0$ and $I_{sh} = 0$. It is also supposed that SSSC1 independently controls its output voltage magnitude and phase values. SSSC2 supplies the real power for SSSC1; as a result V_{c2q} is controlled independently and V_{c2d} depends on V_{c1} which is defined in eq. (13). Fig. 7 shows the results obtained. The controllable region of line-1 is similar to the case where GIPFC is in the loop. However, the controllable region of line-2 is much more limited than in the case where GIPFC is in the loop. In fact this is one of the most important advantages of GIPFC over IPFC.

3. GIPFC Controller

GIPFC's superior operational performance is mainly due to its unique ability to inject a series compensation AC voltage factor with an arbitrary amount of amplitude and phase while sending commands for both systems even with a different voltage level. A shunt converter works in a way that tries to absorb a controlled current I_{sh} and inject it into the line. I_{shd} factor will be provided automatically by forcing real power at the series converter. Since the other current factor, I_{shq}, is reactive, it can be adjusted to any reference value within the converter's controllable limits [1, 2]. The series and shunt converter controller is shown in Fig. 8. Q_{Ref} and P_{Ref} are selected by an external controller (i.e. operator). Having these two values and V_d and V_q factors of V_{22}, appropriate values will be obtained for I_{qRef} and I_{dRef}. The obtained parameters are compared with the measured values from the line (I_d and I_q) and after proper amplification it is used to calculate the angle and amplitude of the series converter output voltage. The controller for SSSC2 is exactly the same as the one for SSSC1.

A voltage limiter is used at the series compensator output to deal with practical constraints which can arise either from system properties or limitations imposed by the devices.

Using up to 24-pulse converters with high power FACTS devices without an AC filter can introduce higher level harmonics, which are not acceptable most of the time. Usually, for 24-pulse converters a high pass filter set to 23^{rd} and 25^{th} harmonics at the transformer side is used. Another option is to use 48-pulse converters (four 12-pulse converters). A system of transformers is used for 24-pulse converters which have 7.5 degrees difference in phase angle. A 48-pulse converter can be used without any AC filter with high power high voltage applications. In this type of converter the output voltage includes harmonics from 48n ± 1 (47, 49, 95, 97 and ...) order with amplitude of 1/48n ± 1 times of the base harmonic. The configuration of the 48-pulse converter implemented in MATLAB/Simulink environment is shown in Fig. 9. It is shown in Fig. 10 how the half-cycle output of a 48-pulse converter is created from sum of the outputs of four 12-pulse converters. The output for 48 and 24 pulse converters (V_{AN}) and their FFT analysis are shown in Fig. 11. It can be seen from Fig. 11 that the THD value for 48-pulse is one half of the THD value for 24-pulse.

4. Simulation results

Fig. 2 shows the modeled system. The modeled STATCOM has 200 MVA nominal power, to enable to provide the power

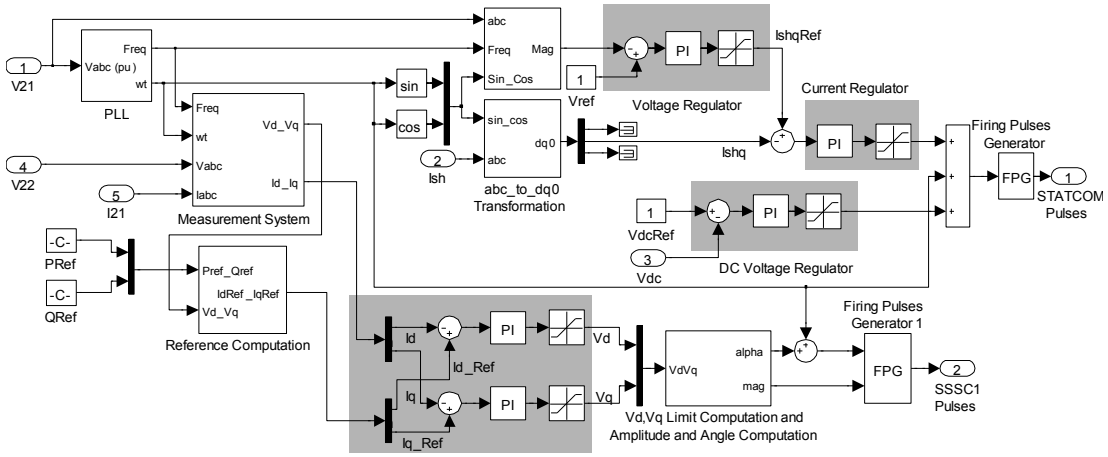

Figure 8: GIPFC Controller

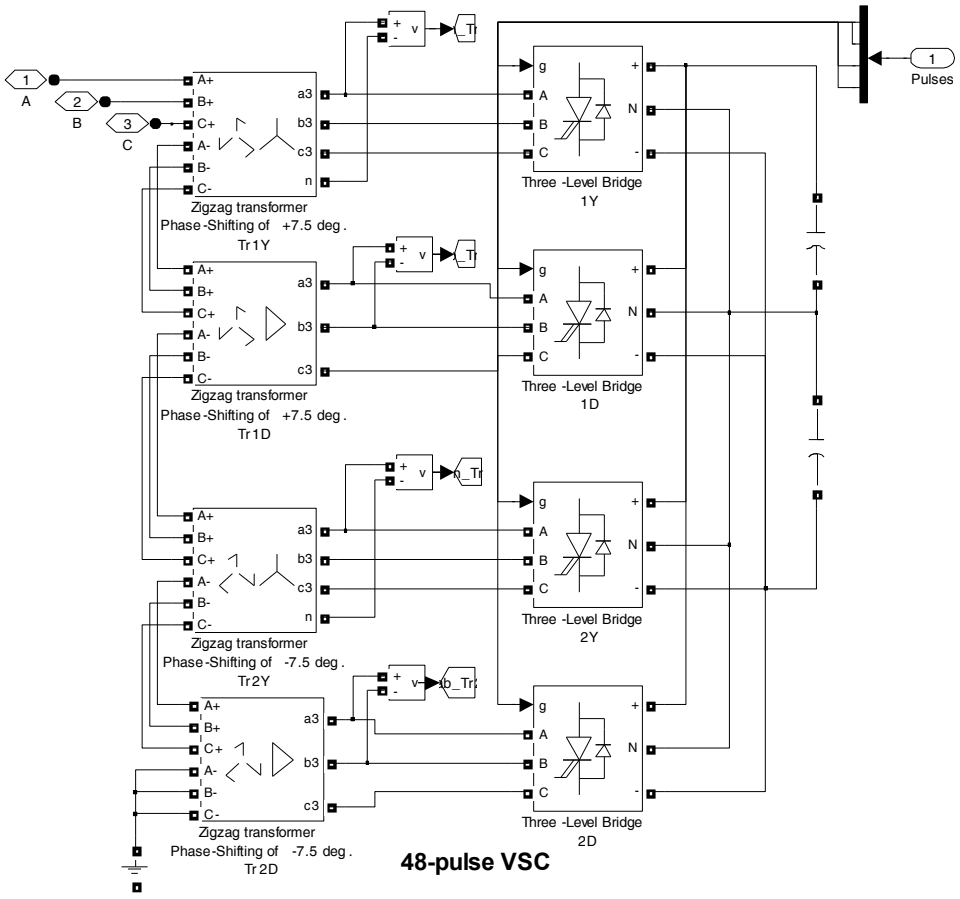

Figure 9: 48 pulse VSC setup in MATLAB/Simulink environment

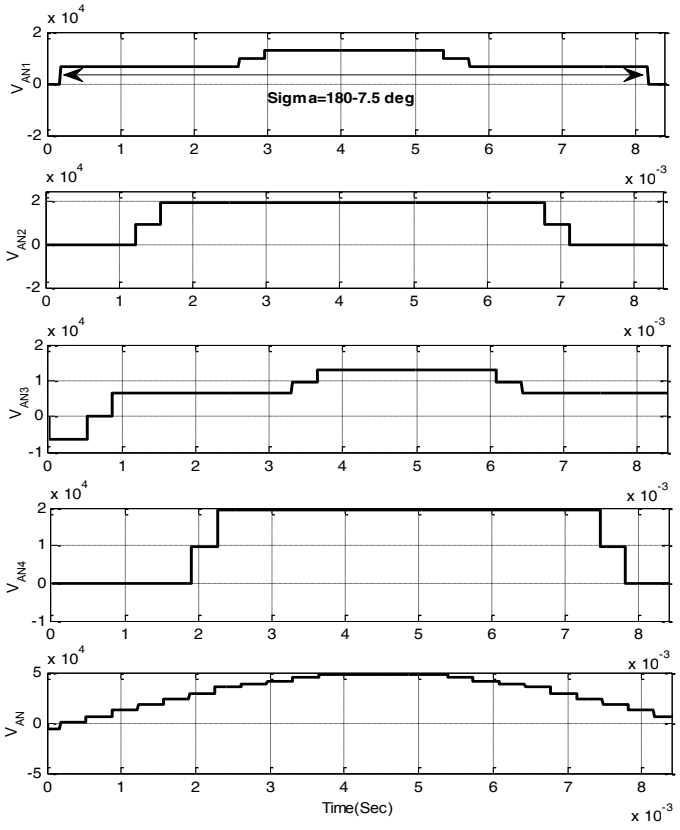

Figure 10: Output of 48 pulse converter

requested by each series converter (100 MVA). 48-pulse VSCs are used to simulate series and parallel converters. The angle difference between the two system is $\delta = 30°$. Simulation results for different working states are presented below.

4.1. GIPFC simulation results

In this operating mode all three converters are used and the GIPFC is in its full operating state. Simulation results are presented in Figures 12–18. Active power at the receiving end of lines 1 and 2 are shown in Figures 12 and 14 respectively. P_{Ref1}, P_{Ref2} and measured active power by the GIPFC are shown in Figures 13 and 15.

It can be seen that the outputs closely follow the referenced inputs. It can be concluded that the transferred power can be controlled across a wide range for both lines. The measured voltage at STATCOM installation point (V_{22}) is shown in Fig. 16. STATCOM independently regulates V_{22} by injecting reactive power. STATCOM should also be able to supply the active power for both series converters, as is shown in Fig. 17. 48-pulse shunt converter (STATCOM) output and V_{22}, I_{ash} are shown in Fig.18. The greater the phase difference is between I_{ash} and converter voltage the greater the greater the active power injected by STATCOM will be. It should also be noted that STATCOM is injecting reactive power to the system because the converter output voltage is greater than V_{22}.

4.2. UPFC

In this state, SSSC1 is not utilized. Power control is similar to GIPFC state with the difference being that in this case the first line remains uncompensated. Simulation results are shown in Figures 19 and 20 for this case. It can be seen from Fig. 20 that the transferred power at the first line has been decreased while it is regulated to a fixed value in the GIPFC case. It should be noted that we have already showed that even the transferred power of the first line can be increased using GIPFC.

4.3. Comparing analytic and simulation results

In this section analytic results are compared to the simulation results. Figures 21 and 22 show P-Q curves for UPFC and SSSC1 containing both analytic and simulated results, respectively. It can be seen that the analytic results are very similar to the simulated results. For example, the injected reactive and active power in GIPFC mode are shown for SSSC1 in Figures 23(a) and 23(b). Combining these two Figures and converting them to P-Q representation will result in the same curve as shown in Fig. 21.

5. Conclusions

GIPFC performance in various operational modes is studied in this paper. It has been shown that GIPFC is capable of controlling transferred power over transmission lines independently for each line. GIPFC is tolerant with regard to faults occurring in a specific part of the controller, i.e., the GIPFC will still continue operating irrespective of a fault in one of its components. It is also shown that there is no need to install additional AC filters if 48-pulse converters are used in GIPFC design. Flexibility and wide range of operation make GIPFC ideal for future works. Future works should investigate how the use of GIPFC impacts transient stability and voltage stability among others.

References

[1] N. G. Hingorani, L. Gyugyi, M. El-Hawary, Understanding FACTS: concepts and technology of flexible AC transmission systems, Vol. 1, IEEE press New York, 2000.

[2] M. El-Moursi, A. Sharaf, Novel controllers for the 48-pulse vsc statcom and sssc for voltage regulation and reactive power compensation, IEEE Transactions on Power systems 20 (4) (2005) 1985–1997.

[3] R. L. Vasquez-Arnez, L. C. Zanetta, A novel approach for modeling the steady-state vsc-based multiline facts controllers and their operational constraints, IEEE transactions on Power Delivery 23 (1) (2008) 457–464.

[4] Z. Huang, Y. Ni, C. Shen, F. F. Wu, S. Chen, B. Zhang, Application of unified power flow controller in interconnected power systems-modeling, interface, control strategy, and case study, IEEE Transactions on Power Systems 15 (2) (2000) 817–824.

[5] J. Bian, D. Ramey, R. Nelson, A. Edris, A study of equipment sizes and constraints for a unified power flow controller, in: Proceedings of 1996 Transmission and Distribution Conference and Exposition, IEEE, 1996, pp. 332–338.

[6] K. K. Sen, Statcom-static synchronous compensator: theory, modeling, and applications, in: Power Engineering Society 1999 Winter Meeting, IEEE, Vol. 2, IEEE, 1999, pp. 1177–1183.

[7] L. Gyugyi, K. K. Sen, C. D. Schauder, The interline power flow controller concept: a new approach to power flow management in transmission systems, IEEE transactions on power delivery 14 (3) (1999) 1115–1123.

[8] J. Chen, T. T. Lie, D. Vilathgamuwa, Basic control of interline power flow controller, in: Power Engineering Society Winter Meeting, 2002. IEEE, Vol. 1, IEEE, 2002, pp. 521–525.

[9] V. Diez-Valencia, U. Annakkage, A. Gole, P. Demchenko, D. Jacobson, Interline power flow controller (ipfc) steady state operation, in: Electrical and Computer Engineering, 2002. IEEE CCECE 2002. Canadian Conference on, Vol. 1, IEEE, 2002, pp. 280–284.

[10] X. Wei, J. H. Chow, B. Fardanesh, A.-A. Edris, A dispatch strategy for an interline power flow controller operating at rated capacity, in: IEEE PES Power Systems Conference and Exposition, 2004., IEEE, 2004, pp. 1459–1466.

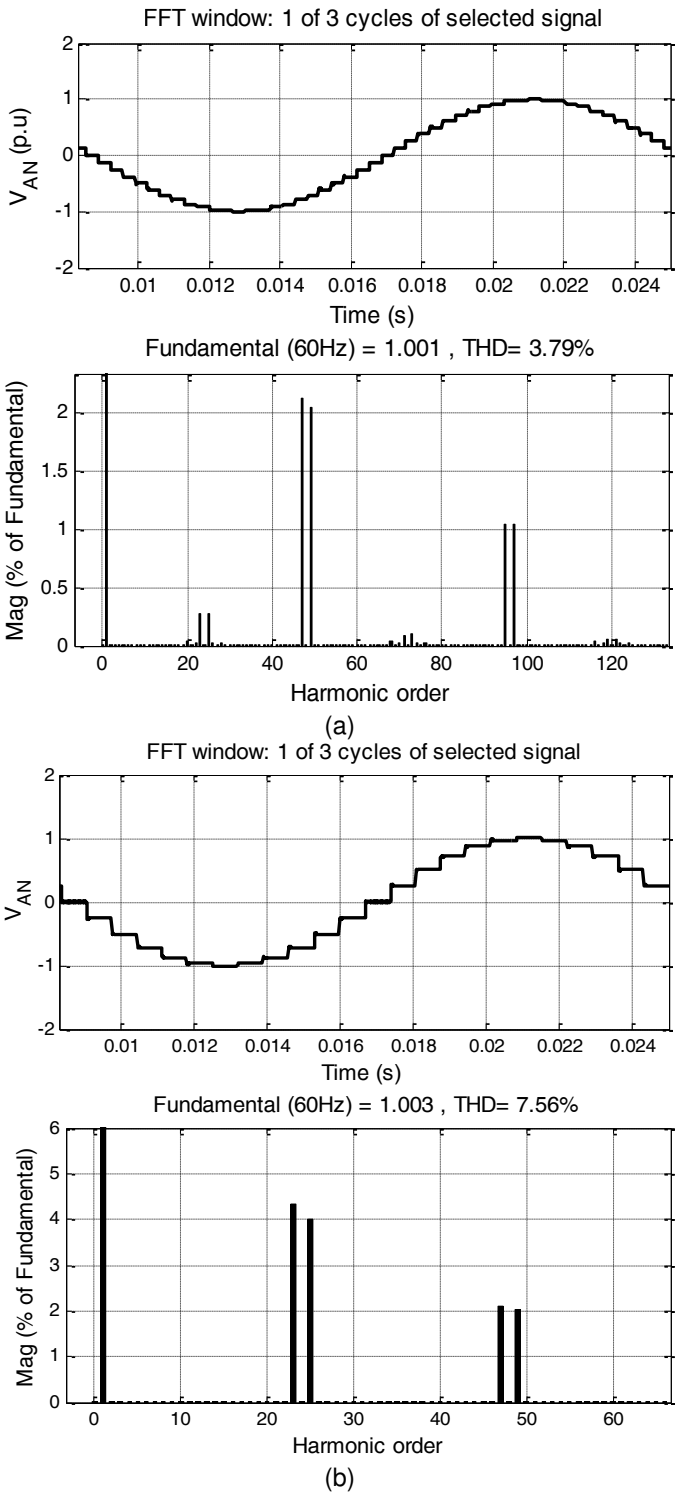

Figure 11: Output of the converter with its FFT analysis (a) 24 pulse, (b) 48 pulse

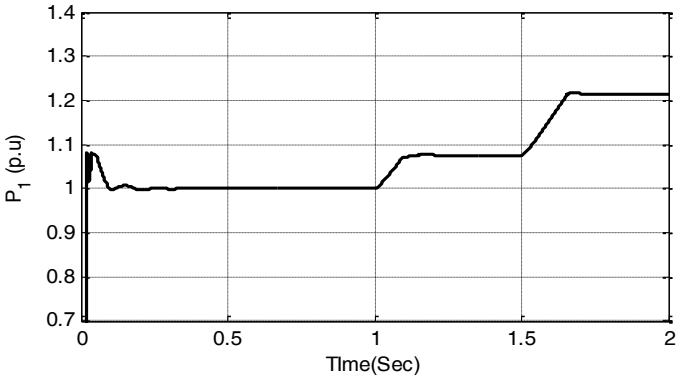

Figure 12: Active power at line 1

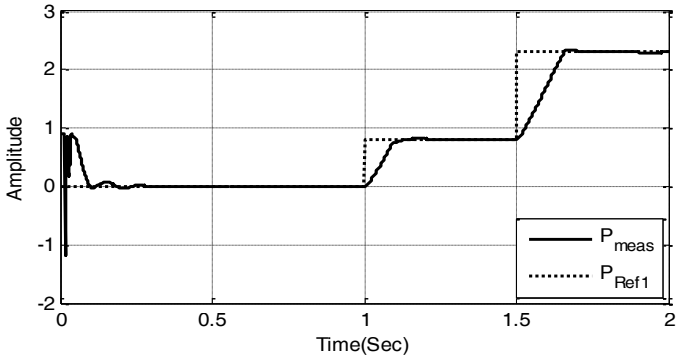

Figure 13: Reference signal for SSSC1 and the measured active power

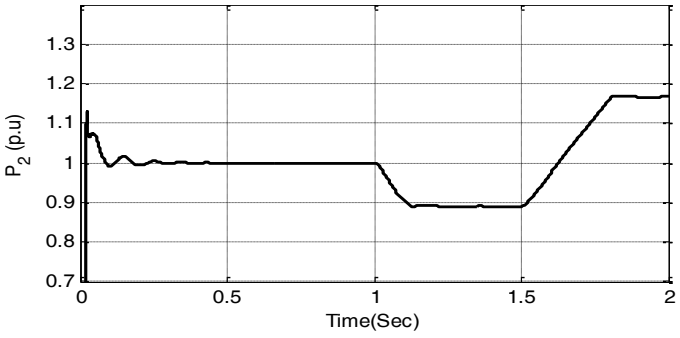

Figure 14: Active power at line 2

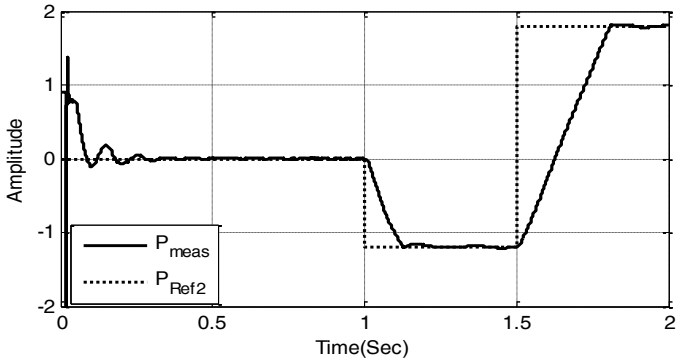

Figure 15: Reference signal for SSSC2 together with measured active power

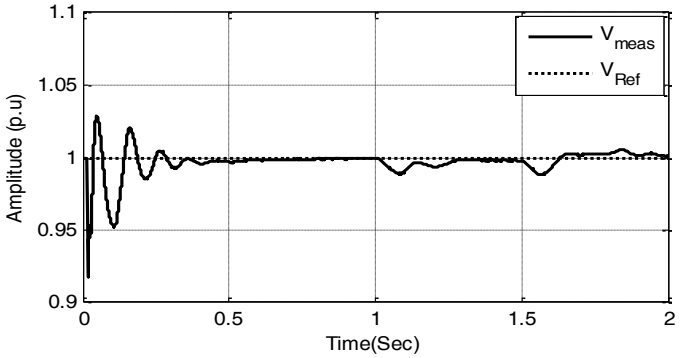

Figure 16: V_{22} and STATCOM V_{ref}

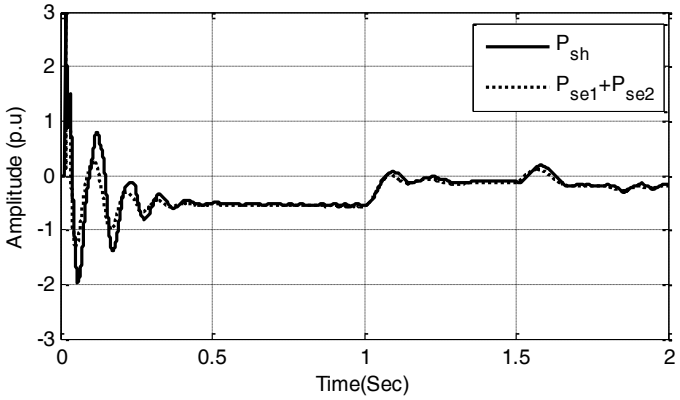

Figure 17: STATCOM active power together with sum of series converters active power

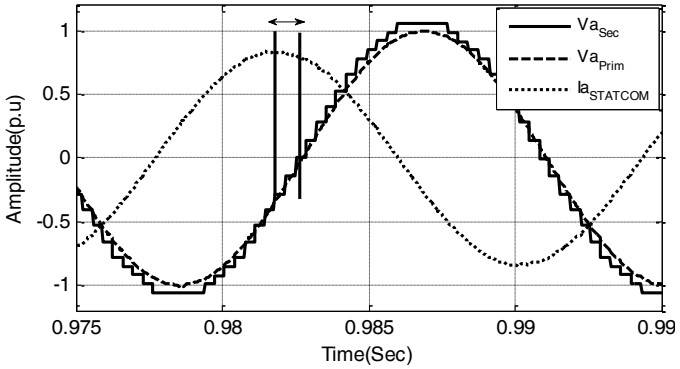

Figure 18: STATCOM 48-pulse converter output together with I_{ash}

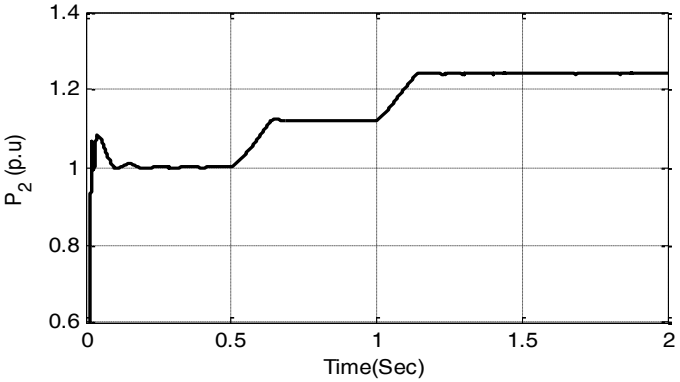

Figure 19: Active power at line 2

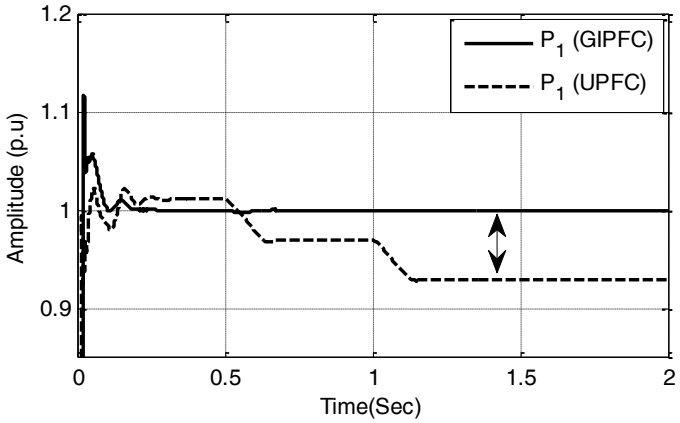

Figure 20: Active power at line 2

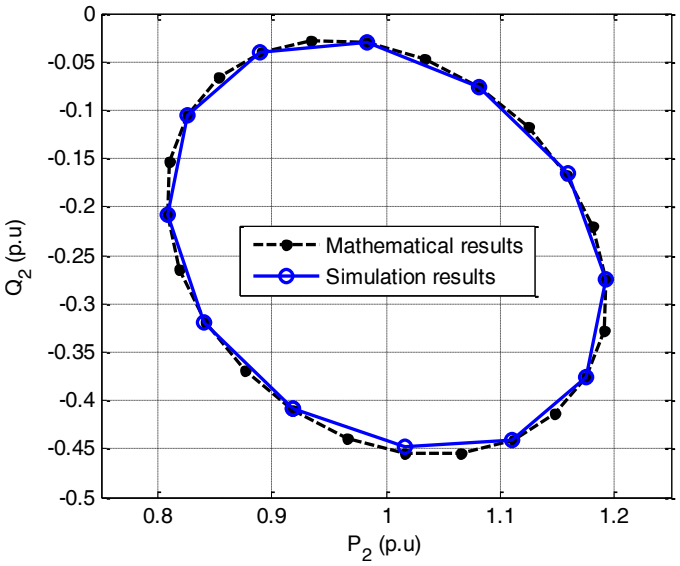

Figure 21: Analytic P-Q curve for different values of injected voltage by UPFC compared to simulation results

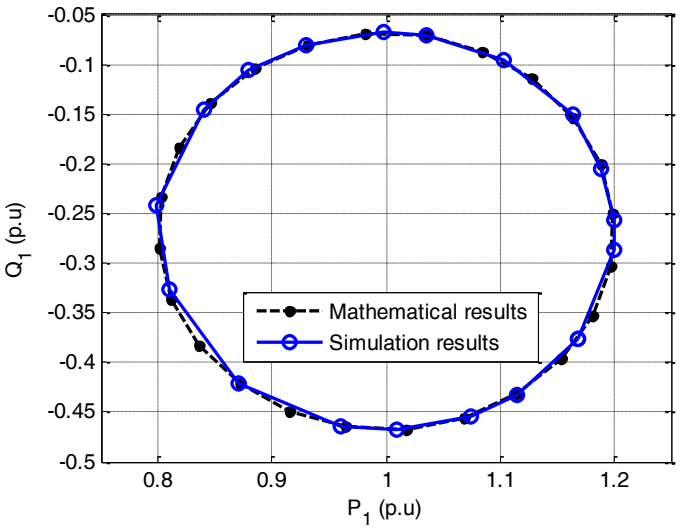

Figure 22: Analytic P-Q curve for different values of injected voltage by SSSC1 compared to simulation results

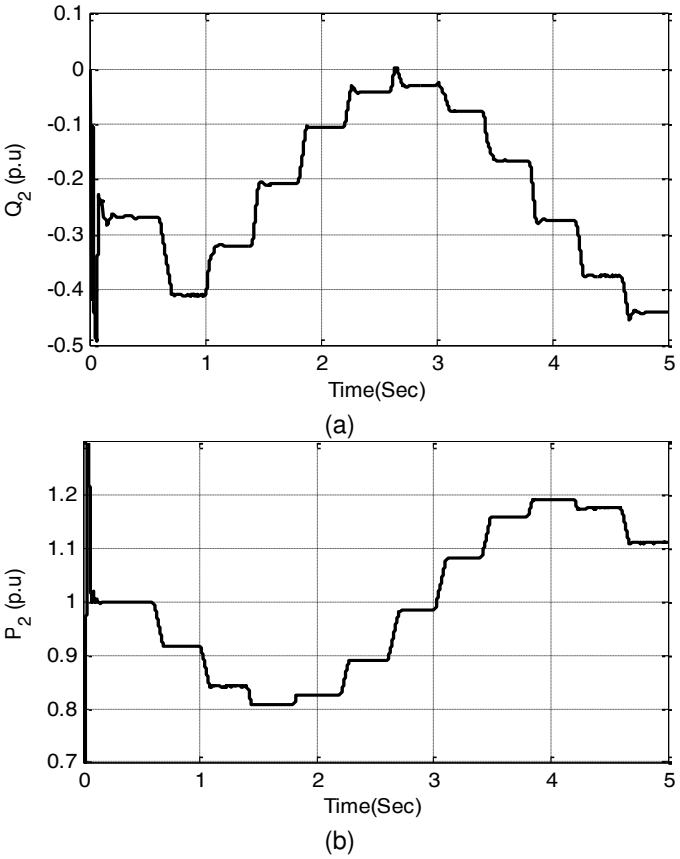

Figure 23: Reactive (a) and active (b) power control at the receiving end using UPFC part of GIPFC